Motions with Inertial and Diurnal Period in a Numerical Model of the Navifacial Boundary Layer[1]

Joseph P. Pandolfo

The Travelers Research Corporation
250 Constitution Plaza
Hartford, Connecticut 06103

ABSTRACT

A model that represents a complex local theory concerning the navifacial[2] planetary boundary layer is presented. The model includes the effects of boundary-layer turbulence in stratified (humidity-dependent and salinity-dependent) flow, of mixing due to wind-generated waves at the naviface, and of cloud-dependent radiative heating throughout the layer.

Solutions for the velocity obtained at selected levels in this boundary layer are demonstrated with two versions of the model. In the first version, the navifacial temperature is considered to be constant in time; in the second version, this temperature is computed from a navifacial heat-budget balance condition under diurnally varying radiational input. Velocities obtained with the first version, like those obtained from the simpler model af Pandolfo and Brown (1967), exhibit (i) a persistent inertial oscillation of significant amplitude in the oceanic layer and (ii) an oscillation of much smaller relative amplitude in the atmospheric layer. Velocities obtained with the second version similarly exhibit persistent inertial oscillations in the oceanic layer; however, in this case they also show a significant diurnal variation in the low-level wind.

The gross agreement of the characteristics derived from the model with some recent observations reported by Fofonoff (1967) is encouraging for further applications of the model.

1. *Introduction.* This paper describes the results of some preliminary experiments with a model that, in its present stage of development, represents a complex local theory intended for the study of the vertical structure in the navifacial planetary boundary layer. The theory is local in that it omits the effects of vertical-transfer processes on horizontal variations in the dependent variables, but it does allow effects in the reverse direction.

1. Accepted for publication and submitted to press 8 May 1969.

2. The words "naviface" and "navifacial" are used with the definition proposed by Montgomery (1969).

A theory such as this should be of considerable interest in an analysis and simulation of phenomena that have apparent characteristic periods of the order of diurnal variations and that have apparent characteristic horizontal wave lengths determined by processes that act over periods of longer duration than the diurnal period so that the horizontal variations may be assumed to be independently prescribable. Thus, a local theory could complement models used for the study of large-scale or long-period phenomena or both. The significance in nature of the restricted set of phenomena that can be studied with such local theories can be judged on the basis of several criteria, such as the relative frequency with which the phenomena are observed (ideally, by quasi-continuous wide-spread observational networks), the relative energy content of the phenomena, and the efficiency in transmitting important physical properties through the navifacial boundary layer.

In this paper, the phenomena discussed are the inertial and diurnal variations in the flow in the vicinity of the naviface——an extension of studies with the simpler model described by Pandolfo and Brown (1967). The model described here is capable of simulating the evolution of many features of the boundary layer that are not described here; these will be discussed in forthcoming papers.

ii a. *The Basic Model.* The model equations take the form

$$\frac{\partial}{\partial t}x_i + V\cdot G_i = \frac{\partial}{\partial z}\left[K_i(Ri,z)\frac{\partial x_i}{\partial z}\right] + A_i \,(i = 1, 2, \ldots 8). \qquad (1)$$

The dependent variables, x_i, and the associated quantities are

i	xi	A_i	i	x_i	A_i
1	u_A	$f[v_A - v_g(z)]$	5	u_w	$f[v_w - v_g(z)]$
2	v_A	$f[u_g(z) - u_A]$	6	v_w	$f[u_g(z) - u_w]$
3	T_A	$\Gamma\partial K_3/\partial z + S_R$	7	T_w	0[3]
4	q	0	8	s	0

The symbols are defined as follows:

u_A eastward component of wind;
v_A northward component of wind;
T_A air temperature;
q specific humidity;
u_w eastward component of current;
v_w northward component of current;
T_w water temperature;

3. This term becomes nonzero in a second version of the model; see § ii d.

s salinity;
V horizontal velocity vector;
G_i horizontal gradient vector for the unknown variable ($G_{1,2,5,6} = 0$);
K_i appropriate eddy-exchange coefficient for the unknown variable;
f Coriolis parameter;
u_g eastward component of the geostrophic velocity;
v_g northward component of the geostrophic velocity;
Γ atmospheric adiabatic lapse rate $\equiv 0.98 \times 10^{-4}\,^{\circ}K\ \mathrm{cm}^{-1}$;
Ri Richardson number;
z the height coordinate, with origin at the naviface; and
S_R temperature source term due to convergence of the infrared radiative flux.

ii b. *Exchange Coefficient Formulae.* Kitaigorodsky (1961) has presented a formulation for the mixing-length variation with distance from a naviface due to the presence of a "mean turbulent wave" at the naviface. The parameters needed to describe the wave are the geometrical properties: δ, the wave steepness (height-to-length ratio); and λ, the wave length. In my model, the length (in cm) is obtained from the solution of wind speed (in cm sec^{-1}) at the 19.5-m level, using the formula

$$\lambda = 28.03 \times 10^{-4} (U_{19.5})^2. \tag{2}$$

This derives from Pierson [1964: eq. (17)] and Pierson et al. [1955: eq. (7)]. Pierson has also suggested that a constant steepness is appropriate for many applications that need parameterization of fully developed wind seas. The value adopted in the present model is $\delta = 0.055$.

Note that the modeling formulae shown above are appropriate for fully developed seas and are applied in the present model to bring the parameterized wave state into immediate and complete adjustment to the low-level wind speed. One would expect this method of parameterization to be unsatisfactory in the simulation of duration-limited or fetch-limited cases. The relevant wave property used to determine the mixing is the vertical gradient of the scalar value of the average orbital velocity in a turbulent wave:

$$S_w(h) = g^{1/2} \delta \left(\frac{\lambda}{2\pi} \right)^{1/2} e^{-h \cdot 2\pi/\lambda}, \tag{3}$$

where g is the acceleration due to gravity and h is the vertical distance from the naviface. In essence, this velocity shear is added to the shear of the mean velocity wherever the second quantity appears in the formulae for the eddy-transfer coefficients and Richardson numbers.

The Richardson number in the atmospheric layer is computed from

$$Ri = \frac{g}{\bar{T}}\left[\frac{\partial T}{\partial z} + \Gamma + .61\,\bar{T}\left(\frac{\partial q}{\partial z}\right)\right]\left[\left|\frac{\partial V}{\partial z}\right| + S_w\right]^{-2}, Ri \leq \frac{1}{|\alpha|}, \tag{4}$$

where α is the Monin-Obukhov constant; see eq. (7).

The Richardson number in the oceanic layer is defined by

$$Ri = -\frac{g}{\bar{\varrho}}\left[\frac{\partial \varrho}{\partial z}\right]\left[\left|\frac{\partial V}{\partial z}\right| + S_w\right]^{-2}, \tag{5}$$

where ϱ is the water density ($\bar{\varrho} \approx 1$ gm/cm^3).

Richardson numbers were not computed at the first grid levels adjacent to the naviface in both the atmospheric and oceanic layers. Therefore, for the computations that follow, Richardson numbers are assumed to be zero at these grid levels.

The density gradient ($\partial\varrho/\partial z$) is given by

$$\frac{\partial \varrho}{\partial z} = 10^{-3} \cdot \frac{\partial \sigma_T}{\partial z} = 10^{-3}\left[\frac{\partial \sigma_T}{\partial T}\frac{\partial T}{\partial z} + \frac{\partial \sigma_T}{\partial s}\frac{\partial s}{\partial z}\right], \tag{6}$$

where the values $\partial\sigma_T/\partial T(s,T)$ and $\partial\sigma_T/\partial s(s,T)$ are obtained by second-degree interpolation from Munk and Anderson (1948: table).

The exchange-coefficient formulae for the atmospheric layer are consistent with the profile formulae discussed by Pandolfo (1966), except that the shear S_w is added to the shear $|\partial V/\partial z|$.

Thus, for inversion conditions, the modified Monin-Obukhov formulae (after Kitaigorodsky) are used:

$$K_{1,2} = k^2\left(z + \frac{\delta\lambda}{2}\right)^2\left(\left|\frac{\partial V}{\partial z}\right| + S_w\right)(1 + \alpha Ri)^2, \tag{7}$$

where $K_{1,2}$ denotes the eddy viscosity, $\alpha = -3.0$, and $k = 0.4$; and

$$K_{3,4} = K_{1,2}, \tag{8}$$

where $K_{3,4}$ denotes the eddy conductivity-diffusivity.

For lapse forced-convection conditions, the nonsimilar formulae are

$$K_{1,2} = k^2\left(z + \frac{\delta\lambda}{2}\right)^2\left(\left|\frac{\partial V}{\partial z}\right| + S_w\right)(1 - \alpha Ri)^{-2}, \tag{9}$$

and

$$K_{3,4} = K_{1,2} \cdot [1 - \alpha Ri]^{-2}, \tag{10}$$

where k and α have the values given above. For lapse free-convection conditions, i.e., for $Ri \leq -0.048$, the formulae are

$$K_{1,2} = K_{3,4} \cdot \left(\frac{3}{C}\right)^{-1/2} \cdot |Ri|^{-1/6}, \tag{11}$$

and

$$K_{3,4} = h\left(z + \frac{\delta\lambda}{2}\right)^2 \left|\frac{g}{\bar{T}}\left(\frac{\partial T}{\partial z} + \Gamma\right)\right|^{1/2}, \tag{12}$$

$$C = 3k^{4/3}h^{-2/3},$$

where h is the Priestley constant. See Pandolfo (1966) for more detail on the formulae and constants used in lapse conditions.

Formulae of this type—for the eddy exchange coefficients—cannot apply under conditions of such extreme stability that the calculated coefficients fall below some physically meaningful minimum value, e.g., the value of the molecular viscosity, conductivity, or diffusivity. There are estimates of such minimum values for the atmospheric boundary layer, but they are several orders of magnitude larger than the values appropriate to laminar flow (Wu 1965, McVehil 1964). There are no such estimates available for the oceanic layer. Therefore, in my model I have imposed minimum values that correspond to the molecular viscosity, conductivity, and diffusivity in the oceanic layer and that are consistent in order of magnitude with estimates available for the atmospheric layer.

Limiting values for the exchange coefficients are imposed in the atmospheric layer:

$$10^4 \leq K \leq 10^7 \text{ cm}^2/\text{sec}; \quad z \geq 100 \text{ m},$$
$$10^2 \leq K \leq 10^7 \text{ cm}^2/\text{sec}; \quad z < 100 \text{ m}.^4$$

The exchange-coefficient formulae used for the oceanic layer are the modified Rossby-Montgomery formulae (after Kitaigorodsky) for stable stratification:

$$K_{5,6} = k_1^2\left(\left|\frac{\partial V}{\partial z}\right| + S_w\right)(1 + 10\,Ri)^{-1/2}, \tag{13}$$

and

$$K_{7,8} = k_1^2\left(\left|\frac{\partial V}{\partial z}\right| + S_w\right)\left(1 + \frac{10}{3}Ri\right)^{-3/2}. \tag{14}$$

For these formulae, Kitaigorodsky assigned an estimated value of $k_1^2 = 0.02$ for the constant k_1.

For unstable stratification, the formulae are identical to the atmospheric-layer lapse-condition formulae, except that the gradient factor, $\partial \ln \varrho/\partial z$, replaces the factor $(1/\bar{T})[(\partial T/\partial z) + \Gamma + .61\,\bar{T}(\partial q/\partial z)]$.

4. Limiting upper values for the atmospheric layer were applied in preliminary experiments in order to minimize the amount of purely numerical error that could be encountered. In subsequent experiments, the grid size and time step were chosen such that the use of this upper limit was unnecessary.

Limiting values of the exchange coefficients are imposed for the oceanic layer under stable conditions, viz.:

$$K_{1,2} \geq 0.14 \text{ cm}^2/\text{sec}$$
$$K_{3,4} \geq 0.0014 \text{ cm}^2/\text{sec}.$$

ii c. *Geostrophic Winds and Currents.* Geostrophic winds at any grid point in the atmospheric layer have been computed from the upper boundary value and from the given horizontal temperature gradients by use of

$$u_g(z) = u_g(H_1) \cdot \frac{T(z)}{T(H_1)} + \frac{g \cdot T(z)}{f} \int_z^{H_1} \frac{1}{T^2} G_{3,y}\, dz, \tag{15}$$

and

$$v_g(z) = v_g(H_1) \cdot \frac{T(z)}{T(H_1)} - \frac{g \cdot T(z)}{f} \int_z^{H_1} \frac{1}{T^2} G_{3,x}\, dz. \tag{16}$$

For the oceanic layer, horizontal density gradients have been computed from prescribed horizontal temperature and salinity gradients (Munk and Anderson 1948: table).

Geostrophic currents at internal grid points have been computed from

$$u_g(z) = u_g(H_2) - \frac{g}{f} \int_{H_2}^{z} \frac{1}{\varrho} \frac{\partial \varrho}{\partial y}\, dz, \tag{17}$$

and

$$v_g(z) = v_g(H_2) + \frac{g}{f} \int_{H_2}^{z} \frac{1}{\varrho} \frac{\partial \varrho}{\partial x}\, dz. \tag{18}$$

In the above formulae, H_1 denotes the upper boundary and H_2 the lower boundary.

ii d. *Boundary and Navifacial Conditions and Initial Values.* For the upper boundary, the values of wind, temperature, humidity, and geostrophic wind have been prescribed throughout the period of integration.

For the lower boundary, values of current, temperature, salinity, and geostrophic current have been prescribed.

Boundary values of wind and current were equal to input geostrophic winds and currents at the boundary.

For the naviface, the temperature has been prescribed. The navifacial velocity value has been computed from the conditions

$$V_A = V_w,$$
$$\varrho_A K_A \frac{\partial V_A}{\partial z} = \varrho_w K_w \frac{\partial V_w}{\partial z}.$$

The navifacial humidity value has been computed as the saturation value at the navifacial temperature. The navifacial salinity value has been computed from the condition

$$\varrho_w K_w \frac{\partial ln s}{\partial z} = \frac{E}{1-s},$$

where

$$E = \varrho_A K_A \frac{\partial q}{\partial z}\left(\frac{gm\, H_2O}{cm^2\, sec^1}\right);$$

q and s are in gm/gm.

Initial values are given at all grid points except at the naviface, where only the initial temperature is given. Other initial navifacial values have been computed from the conditions given above.

In a second version of the model (see § iii c), at each time step the prescribed navifacial temperature has been replaced with a temperature that has been computed iteratively from the following equation:

$$\left.\begin{aligned} 0 &= SR_s + R_A - LE(T_I) - \sigma T_I^4 - \\ &- \varrho_A c_p K_A \left[\left(\frac{\partial T}{\partial z}\right)_{+0} + \Gamma\right](T_I) - \varrho_w c_w K_w \left(\frac{\partial T}{\partial z}\right)_{-0}(T_I); \end{aligned}\right\} \quad (19)$$

the symbols are defined as:

R_A	the total atmospheric (infrared) radiative flux incident on the interface;
SR_s	the amount of solar radiation absorbed in the uppermost half-grid layer of the oceanic sublayer;
L	latent heat;
σ	the Stefan constant;
$(\partial T/\partial z)_{+0}$	the vertical temperature gradient in the lowest atmospheric grid layer;
K_A	the atmospheric eddy conductivity at the midpoint of this layer;
$(\partial T/\partial z)_{-0}$	the vertical temperature gradient in the uppermost oceanic grid
K_w	layer; and the eddy conductivity at the midpoint of this layer.

As shown in the heat-balance equation, three terms depend implicitly on the balance temperature (T_I); one of the terms explicitly contains the fourth power of this quantity and two terms are independent of T_I.

In this second version of the model, the initial value of the temperature has not been given; additional source terms representing the amount of solar radiation absorbed at each grid level and time step are included in the terms A_3, A_7 in eqs. (1). Note that, in this version, A_7 no longer has to remain zero at all times. The infrared calculations use model-derived temperature, humidity, and pressure soundings (hydrostatically computed from prescribed pressure

at one atmospheric grid level) within the modeled layer and prespecified atmospheric soundings above this layer. The model has used the corrected Brooks method suggested by Atwater (1966). The solar radiation has been computed by using a method of Fritz (1951), with a linearly extended transmission table beyond air mass 4.5. It is assumed that the navifacial albedo varies with the zenith angle according to an empirical expression fitting observations of solar reflection given by Sverdrup et al. (1942: table 26): $r_s = -1.39 + 4.67 \tan Z$, where r_s is the albedo and Z is the solar zenith angle.

Absorption from solar radiation in the atmosphere has been computed by using an empirical formula given by Mügge and Möller (1932); absorption in the oceans has been computed by applying absorption coefficients from Sverdrup et al. (1942: table 27).

ii e. *Numerical Integration of the Conservation Equations.* The finite-difference analogues to the diffusion eqs. (1) have been adapted from an implicit three-time level scheme given by Richtmyer and Morton (1967: table 8.1). Scheme 9 was selected because of the irregular nature of the initial data to be used in the integration. An extensive discussion by Gerrity of the numerical scheme is available on request (Pandolfo et al. 1967).

iii a. *The Input Data.* Basic climatological data obtained at Atlantic Ocean station "Echo" (approximately 33°N, 47°W) for February have been used for the first set of preliminary experiments (see Table I).

Zero values were taken for the remaining required input parameters, viz., the horizontal gradient of oceanic temperature and salinity, the horizontal gradient of atmospheric humidity, and the geostrophic current.

Table I. First set of preliminary experiments, using basic climatological data from Atlantic Ocean Station "Echo" for February.

Input Parameter	Value	Source
850-mb gs wind	u = 865 cm/sec v = 111 cm/sec	Jacobs 1957
1000-850-mb mean horizontal temp. gradient (from 1000-mb, 850-mb pressure charts)	$\partial T/\partial x = -3.78 \times 10^{-8}$ °/cm $\partial T/\partial y = -7.55 \times 10^{-8}$ °/cm	Jacobs 1957
Navifacial temp.	292.49 °K	U.S. Weather Bureau 1959
850-mb temp.	279.40 °K	Starr and Frazier 1965
850-mb specific humidity	5.48 g/kg	Starr and Frazier 1965
temp.-humidity profiles above 850 mb		Starr and Frazier 1965
400-m salinity	36.250‰	Defant 1961
200-m temp.	290.96 °K	Sverdrup et al. 1942
400-m temp.	290.16 °K	Sverdrup et al. 1942

Initial profiles for most of the experiments were constructed by linear interpolation in height (depth) between the levels for which climatic values were available and the levels (intermediate) for which values were assumed. No assumed intermediate value was required for the temperature. It is assumed that the wind was zero at the lowest atmospheric grid level above the naviface. The currents were assumed to be zero at all levels. The navifacial humidity was assumed to be equal to the saturation value at the navifacial temperature. The navifacial salinity was taken at 36.8‰, as indicated by Defant (1961) in his surface-salinity chart.

For the heat-balance version of the model, the initial declination and hour angles were those that correspond to 0930 local sun time, 13 February. All radiation computations were carried out for cloudless conditions.

For these integrations, the upper boundary was placed at +1500 m, the lower boundary at −400 m. Intermediate grid levels were, in ascending order, −300, −200, −100, −75, −60, −55, −50, −45, −40, −35, −30, −25, −20, −15, −10, −5, −1, 0, 1, 6, 25, 75, 125, 250, 500, and 1000, with all heights (depths) in meters. The time step used was 3 minutes, and the total period of integration included 2400 time steps. An integration with the surface heat-balance computation required approximately four minutes on a Sperry Rand 1108 computer.

iii b. *Solutions with the Prescribed Steady Navifacial Temperature.* Note that the upper boundary conditions given in § ii d do not correspond exactly with those used in the linear models of Pandolfo and Brown (1967) because the velocity in the numerical model remains constant in time. However, the results are comparable in a qualitative sense in that the apparent inertial oscillation of the atmospheric layer in both models is of negligible amplitude relative to the geostrophic flow in this layer (of order 1% in the linear model and of order 0.1% in the numerical model). Fig. 1 shows the evolution of the u-component in the numerical solution at grid levels +6 m and −5 m (with 0 m taken at the naviface). Although the fluctuations at these two levels are perfectly coherent, the kinetic energy in the atmospheric fluctuation is at least four orders of magnitude smaller than that in the oceanic fluctuations.

The amplitude of the oceanic velocity fluctuation is of the order of 1% of the geostrophic wind speed and is at least as large as the mean drift, again in qualitative agreement with the predictions of the linear model.

The two model solutions are also qualitatively consistent in that the amplitude of the inertial oscillations in each solution decreases for the oceanic layer, which is assumed to be of finite depth (see Pandolfo and Brown 1967: fig. 4).

Pandolfo and Brown [1967: fig. 5, eqs. (18), (19)] have shown that it is impossible to calculate a simply defined decay rate for the linear (constant K) model. Therefore, extrapolation of the solution for the nonlinear model in Fig. 1 beyond the period of numerical integration would be speculative at best.

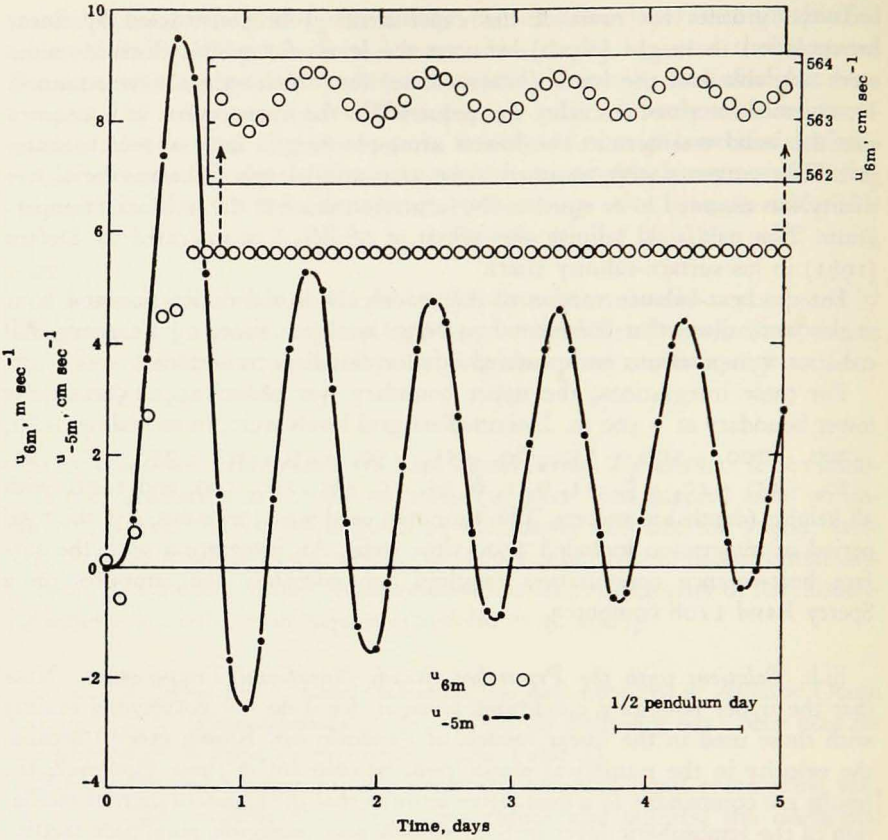

Figure 1. The u-component of velocity shown as a function of time over the period of numerical integration at grid levels + 6 m and − 5 m. Note expansion in scale of the time series for the wind at about one day. The time series represents solutions obtained with the first version of the boundary-layer model.

It does appear that some steady state, in which all of the kinetic energy of the oceanic motion is found in the mean drift, might eventually be reached, but there is no apparent physical reason for this result to be characteristic of the nonlinear model.

iii c. *Solutions with the Computed Heat-balance Temperature.* In the model solutions, inclusion of the navifacial heat-balance components produces significant diurnal variations in navifacial temperature; these variations are accompanied by diurnal variations in the Richardson number and, consequently, in eddy viscosity. Fig. 2 shows the model-generated navifacial temperature variations during the fifth day of integration; Fig. 2 also shows the accompanying Richardson number variations at levels + 3.5 m and − 3.0 m.

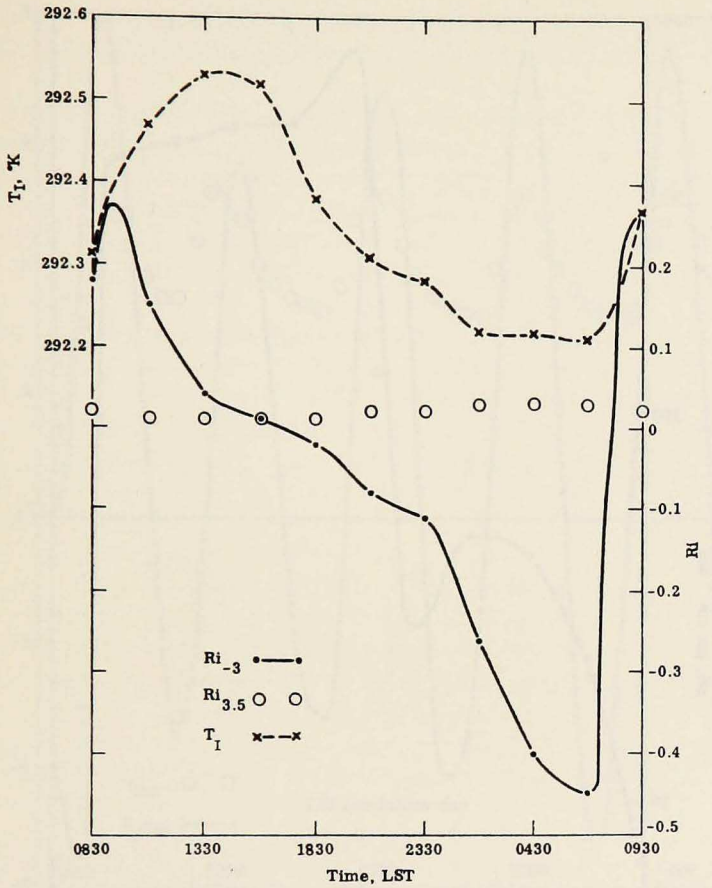

Figure 2. Richardson number (Ri) and interface temperature (T_I) shown as a function of time over the final 25 hours of the period of integration. The Richardson number is shown for grid levels $+3.5$ m and -3 m. The time series represents solutions obtained with the second version of the boundary-layer model.

The relatively large diurnal range of the Richardson number in the upper oceanic layer is of interest. This range is apparently generated by solar heating in the late morning and by destabilization at night due to radiative cooling at the naviface. The accompanying diurnal variation in the lower atmospheric layer is small by comparison, with the layer being slightly less stable through mid-day than during the night. Associated dynamic eddy-viscosity variations are shown in Fig. 3; as expected from the Richardson-number curves, there is a much larger range of diurnal variation in the upper oceanic layer than in the lower atmospheric layer, with maximum viscosities at the time of maximum destabilization of the respective layers. (However, a secondary oceanic viscosity maximum may accompany the afternoon maximum in wind and current speeds.)

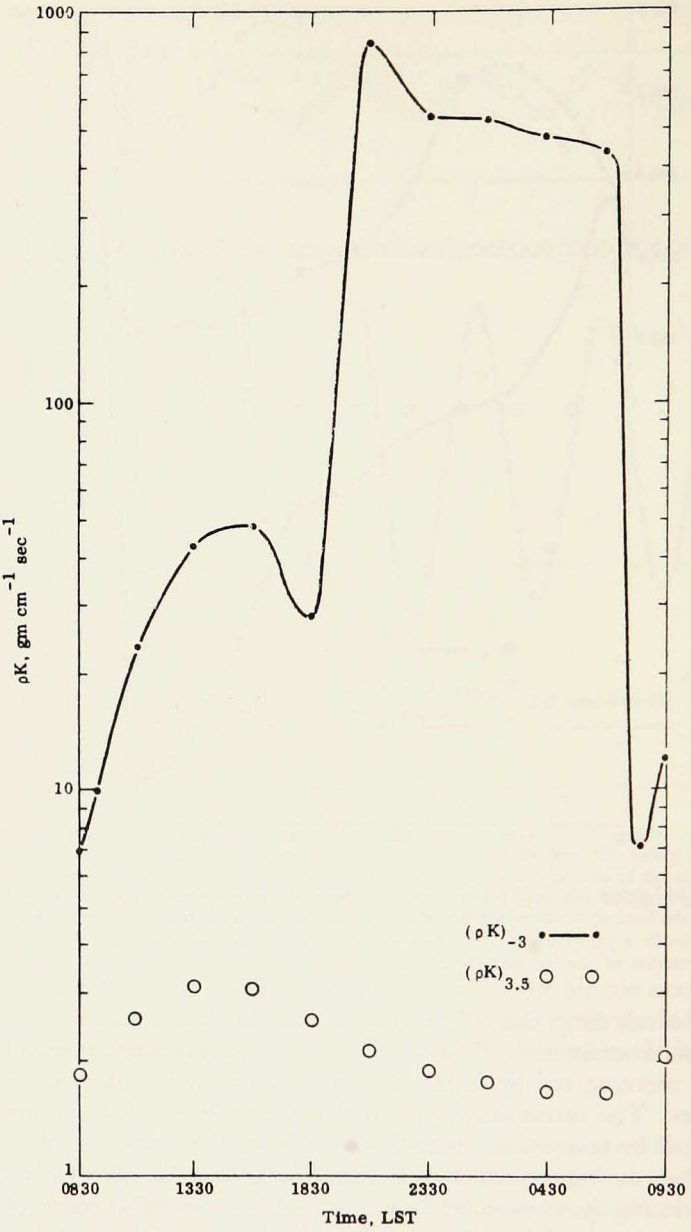

Figure 3. Dynamic eddy viscosity (ϱK) shown as a function of time over the final 25 hours of the period of integration. The time series represents solutions obtained with the second version of the boundary-layer model.

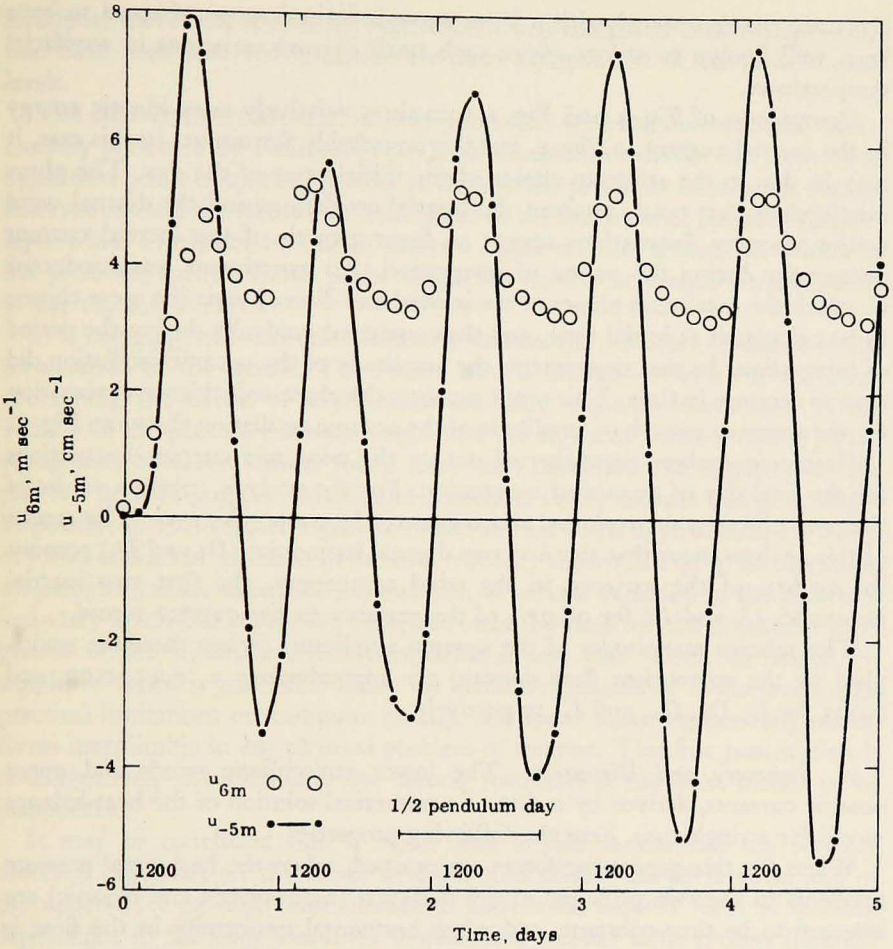

Figure 4. Same as Fig. 1, but with solutions obtained from the second version of the boundary-layer model.

In view of the diurnal viscosity curves shown in Fig. 3, the behavior of the velocity in the two layers is paradoxical, at least at first glance. In spite of the apparently large range of viscosity in the upper oceanic layer, the inertial period still persists as the dominant period of fluctuation in this layer (see Fig. 4). On the other hand, the low-level wind now shows a pronounced, though not simple, diurnal oscillation. The range in this variation (2 to 3 m/sec) is in qualitative agreement with the diurnal range recently observed in the eastern trade-wind region (Augstein 1967). The temperature range shown in Fig. 2 (0.3°C) is in reasonable agreement with the range given by Defant (1961) for the same general region of the ocean. Future model studies may explain why

the trade winds respond with a large enough diurnal range of speed to have been well known to sailors, given such small diurnal variations in navifacial temperatures.

Comparison of Fig. 4 and Fig. 1 does show relatively *more* kinetic energy in the inertial current in Fig. 4, but this is probably fortuitous; in this case, it may be due to the arbitrary choice of the initial hour of the day. The phase relationships that result between the inertial oscillations and the diurnal wind and/or viscosity fluctuations appear to favor growth of the inertial current component during the period of integration. An experiment was conducted in which the maximum phases of the inertial and diurnal variation were chosen to be coincident at initial time, and thus separated gradually during the period of integration. In that experiment, the amplitude of the oceanic oscillation did tend to decrease in time. This result supports the phase-coincidence explanation for the apparent growth of amplitude of the oceanic oscillation shown in Fig. 4.

Harmonic analyses were carried out on the wind and current fluctuations for the final day of numerical integration. For the analysis, solution values of the u-components were plotted and connected by a smooth curve. The results of this analysis show that the first two diurnal harmonics (D_1 and D_2) account for 99.6% of the variance in the wind component, the first two inertial harmonics (I_1 and I_2) for 98.7% of the variance in the current record.

The relative magnitudes of the squared amplitudes (when these are multiplied by the appropriate fluid density) are approximately 1, 0.25, 0.02, and 0.005 for I_1, D_1, D_2, and I_2, respectively.

iv. *Summary and Discussion.* The lower atmospheric winds and upper oceanic currents, derived by means of a numerical solution of the heat-balance model for a single case, have the following properties.

When the tide-generating forces are omitted, when the horizontal pressure gradients in the two principal model sublayers (atmospheric and oceanic) are assumed to be time-constant, and when horizontal uniformity in the flow is assumed, the dominant energy-containing modes of flow (other than the mean mode) are the inertial mode in the current and the diurnal mode (with its harmonics) in the wind. No diurnal mode is evident in the current, even though there is in the upper oceanic layers a diurnal range of the source term, A_7. The amplitude of A_7 is about 0.5°/day at the -5-m grid level and comparable to the range in the source term, A_3, at the 6-m level (1°/day). Compared with the lower atmospheric level (Fig. 2), the upper oceanic layer exhibits greater instability (as measured by the Richardson number) through a large part of the day and a much larger range of stability variation. These characteristics would not, *a priori*, appear to favor the dominance of the diurnal mode in the wind and its absence in the current, as is shown by the model solutions. The range in fluctuation at these periods is significant when compared with the mean and longer-period transient modes in the numerical-model

solutions; moreover, it remains significant when compared with typical values that have been observed in nature for other components of the flow at these levels.

The characteristics are qualitatively consistent with the observational results recently presented by Fofonoff (1967); his results have shown the presence of significant peaks of spectral density at the inertial period in fixed-point current observations and the absence of these peaks in the spectrum of observed surface-layer wind. Furthermore, one of the two observed wind records for which he has presented spectra shows peaks in spectral density at periods corresponding to 24, 12, and 8 hours.

It is not suggested that this qualitative consistency validates all details in the formulation of the model. The reader who is unfamiliar with the literature concerning the effects of stratification on eddy exchange coefficients in the vicinity of the planetary surface might find the algebraic form of eqs. (7)–(14) repugnant; however, similar forms have been developed and applied over the past few decades (e.g., see Munk and Anderson 1948, Estoque 1963). It might be possible to find simpler algebraic formulae that could approximate the range of forms of diurnal variation in the eddy viscosity shown in Fig. 3; furthermore, they might provide satisfactory simulation of natural variation in the planetary boundary layer. However, the computer must be used for the numerical integration of the nonlinear diffusion equation in any case. Thus, the search for simplified forms is justifiable either on aesthetic grounds or in the event that practical limitations on computer storage and speed make algebraically ornate forms inapplicable in *any* physical problem of interest. The first justification is not objectively debatable and the second justification has been shown to be inapplicable.

It may be concluded that a model that is able to simulate the recently observed difference in the mode of oscillation of the low-level wind and of the upper-level current must include at least some explicit form of stability dependence in the eddy viscosity; it must also include some process (implicit or explicit) for the generation of stability variations.

The diurnal mode, because of its effect on low-level wind variations, should be significant in determining the values and the ranges in variation in the vertical eddy fluxes of horizontal momentum, heat, and water vapor through the atmospheric boundary layer. The relationship between the low-level wind and one of these fluxes, as indicated in the model solutions, has been briefly described (Pandolfo 1968). The fact that there is such a relationship has been indicated by repeated observational studies over the sea surface.

It may be concluded, therefore, that the phenomena discussed here are of importance when judged according to the three criteria proposed at the beginning of this paper. The results obtained by integration from this single set of initial and boundary conditions appear to satisfactorily simulate, in some important respects, the characteristics seen in the relatively few samples of fixed-

point observational data available at present. Furthermore, experiments with this type of model under varying input parameter values appear to be desirable in preparation for, and in conjunction with, the expected acquisition of more data of this type in the future.

Acknowledgments. This work has been supported by the Sea-Air Interaction Laboratory of ESSA [contract E-120-67(N)] and facilitated by the cooperation and patience shown by the laboratory director, Feodor Ostapoff. M. A. Atwater has made an important contribution in the adaptation of the radiative and heat-budget calculation schemes, and J. A. Sekorski has written the computer programs. The manuscript was typed by M. G. Atticks.

REFERENCES

Atwater, M. A.
1966. Comparison of numerical methods for computing radiative temperature changes in the atmospheric boundary layer. J. appl. Meteor., *5*: 824–831.

Augstein, Ernst
1967. Fine structure analysis of air-temperature and humidity in the lower 200 m of the Atlantic Trade Wind region. *Paper presented at* XIVth General Assembly IUGG, IAMAP, Lucerne Switzerland, September 25–October 7, 1967. 1 p.

Defant, Albert
1961. Physical oceanography. Pergamon Press, N.Y., 2 vol.; 1327 pp.

Estoque, M. A.
1963. A numerical model of the atmospheric boundary layer. J. geophys. Res., *68*: 1103–1113.

Fofonoff, N. P.
1967. Ocean variability – Atlantic. *Paper presented at* 134th Annual Meeting, AAAS, New York. 13 pp.

Fritz, Sigmund
1951. Solar radiant energy and its modification by the earth and its atmosphere. Compendium of Meteorology, Amer. Meteor. Soc., Boston. pp. 13–33.

Jacobs, I. S.
1957. 5-resp. 40-year monthly means of the absolute topographies of the 1000-mb, 850-mb, 500-mb, and 300-mb levels . . ., Inst. Meteorol. Geophys., Freien Univ., Berlin. 199 pp.

Kitaigorodsky, S. A.
1961. On the possibility of theoretical calculation of vertical temperature profile in upper layer of the sea. Bull. (Izvestia) acad. Sci., USSR, Geophys. Ser., *3*: 313–314.

McVehil, G. E.
1964. Wind and temperature profiles near the ground in stable stratification. Quart. J. roy. Meteor. Soc., *90*: 136–146.

Montgomery, R. B.
1969. The words naviface and oxyty. J. mar. Res., *27*: 161–162.

MÜGGE, R., and FRITZ MÖLLER
1932. Uber abkuhlungen in der freien Atmosphare infloge der langwelligen Strahlung des Wasserdampfes. Meteorolog. Z., *41*: 95.

MUNK, WALTER, and E. R. ANDERSON
1948. Notes on a theory of the thermocline. J. mar. Res., *7*: 276–295.

PANDOLFO, J. P.
1966. Wind and temperature profiles for constant-flux boundary layers in lapse conditions with a variable eddy conductivity to eddy viscosity ratio. J. atmos. Sci., *23*: 495–502.
1968. A numerical model of the atmosphere-ocean planetary boundary layer. *Paper presented at* WMO/IUGG Symp. on Numerical Weather Prediction, Tokyo, Japan, 26 November–4 December. II. pp. 31–40.

PANDOLFO, J. P., and P. S. BROWN
1967. Inertial oscillations in the Ekman layer containing a horizontal discontinuity surface. J. mar. Res., *25*: 10–28.

PANDOLFO, J. P., P. S. BROWN, and J. P. GERRITY
1967. Preliminary experiments with a numerical model of the atmosphere-ocean planetary boundary layer. Final Report 7044S258, Contract Cwb-11315, The Travelers Research Center, Inc., Hartford, Conn. 86 pp.

PIERSON, W. J.
1964. The interpretation of wave spectrums in terms of the wind profile instead of the wind measured at a constant height. J. geophys. Res., *69*: 5191–5204.

PIERSON, W. J., GERHARD NEUMANN, and RICHARD JAMES
1955. Practical methods for observing and forecasting ocean waves by means of wave spectra and statistics. H. O. Publ. 603, U.S. Navy Hydrographic Office, Washington, D.C. 284 pp.

RICHTMYER, R. D., and K. W. MORTON
1967. Difference methods for initial value problems. 2nd ed., Interscience Publ., John Wiley & Sons, N.Y. 405 pp.

STARR, V. P., and H. M. FRAZIER
1965. An arrangement of data for dynamical studies of the atmosphere. Data processing in meteorology, World Meteorological organization, Geneva; Techn. Note 73: 3–39.

SVERDRUP, H. U., M.W. JOHNSON, and R. H. FLEMING
1942. The oceans. Prentice-Hall, Inc., N.Y. 1087 pp.

U.S. WEATHER BUREAU
1959. Climatological and oceanographic atlas for mariners. Vol. 1, The North Atlantic. U.S. Navy Hydrographic Office, Washington, D.C. 189 pp.

WU, S. S.
1965. A study of heat transfer coefficients in the lowest 400 meters of the atmosphere. J. geophys. Res., *70*: 1801–1808.